GEOPHYSICAL RESEARCH LETTERS, VOL. 34, L07404, doi:10.1029/2006GL029200, 2007

Ultrasonic properties of granular media saturated with DNAPL/water mixtures

J. B. Ajo-Franklin,[1,2] J. T. Geller,[3] and J. M. Harris[4]

Received 23 December 2006; revised 13 February 2007; accepted 19 February 2007; published 11 April 2007.

[1] We present the results of four experiments investigating the ultrasonic properties of granular materials partially saturated with trichloroethylene (TCE), a dense non-aqueous contaminant. P-wave velocity measurements were made under *in situ* effective stress conditions using a pulse transmission cell at ≈250 kHz. Two synthetic samples and two natural aquifer cores were fully saturated with water and then subjected to an axial injection of TCE. The resulting measurements show reductions in P-wave velocity of up to 15% due to contaminant saturation. A theoretical model combining Gassmann fluid substitution and Hill's equation was used to estimate the effects of DNAPL saturation; this model underpredicted observed reductions in velocity at high TCE saturations. A linear relationship, expressed in terms of volumetric contaminant fraction, provided an excellent empirical fit to the laboratory measurements. **Citation:** Ajo-Franklin, J. B., J. T. Geller, and J. M. Harris (2007), Ultrasonic properties of granular media saturated with DNAPL/water mixtures, *Geophys. Res. Lett.*, *34*, L07404, doi:10.1029/2006GL029200.

1. Introduction

[2] The *in situ* detection and delineation of toxic contaminants is an on-going challenge for scientists responsible for environmental site remediation. Dense non-aqueous phase liquids or DNAPLs are a class of fluids which include several problematic industrial contaminants including the chlorinated solvent trichloroethylene (TCE) [*Pankow and Cherry*, 1996]. Multiple geophysical techniques have been proposed for DNAPL detection in shallow subsurface environments [*Romig*, 2000]. However, most methods lack the spatial resolution and/or sensitivity for the characterization of small DNAPL lenses or pools. High-resolution borehole seismic methods may have sufficient resolution in some geological scenarios when appropriate source frequencies and experiment geometries are used. While previous seismic imaging experiments have targeted regions of DNAPL contamination [*Temples et al.*, 2001], to date no core-scale ultrasonic measurements have been performed on DNAPL-saturated aquifer materials, a prerequisite for the calibration of relevant rock-physics models.

[3] We present the results of four experiments investigating the ultrasonic properties of granular materials partially saturated with TCE. These measurements provide constraints on the seismic signature of partial DNAPL saturation. Two natural aquifer samples and two synthetic glass bead packs of differing porosities were examined. All samples were initially water saturated before being subjected to an axial injection of TCE. TCE is a colorless fluid with a high density (1464 kg/m^3), a low P-wave velocity (1050 m/s [*Nath and Saini*, 1990]), and a low viscosity (0.56×10^{-3} Poise [*Mercer and Cohen*, 1990]) with respect to water at 20°C. TCE has a low aqueous solubility (1100 mg/L [*Montgomery*, 1991]) but is tightly regulated by the EPA with a maximum allowable concentration of 0.005 mg/L in drinking water.

[4] Ultrasonic pulse transmission measurements were acquired during the injection of TCE into the granular samples allowing determination of P-wave velocity as a function of DNAPL saturation. Maximum TCE saturation varied between 22% and 59% for the four samples. Since only water and TCE were used as saturating fluids, our results are most relevant to characterization of DNAPLs in the saturated zone. The resulting velocity estimates show a reduction in P-wave velocity as a function of DNAPL saturation. The largest observed velocity decrease was 15% at a TCE saturation of 59%. A combination of Gassmann fluid substitution and Hill's equation was used to estimate the effects of DNAPL saturation but underpredicted the observed decrease in velocity at high TCE levels. A linear model, expressed in terms of volumetric contaminant fraction, provided an excellent empirical fit to our measurements across all samples.

1.1. Principles

[5] The key parameters for determining the seismic signature of fluid saturation are the fluid's compressional wave velocity ($V_{p_{fl}}$) and density (ρ_{fl}) which can be directly related to fluid bulk modulus ($K_{fl} = V_{p_{fl}}^2 \rho_{fl}$). Fluids with a high bulk modulus stiffen porous materials; at higher frequencies viscous losses can be generated due to motion of the saturating fluid with respect to the porous matrix. Biot-Gassmann theory [*Biot*, 1956] describes the effects of pore fluids on the bulk elastic properties of porous materials. The theory does not attempt to predict rock properties from *ab initio* information concerning phase properties and geometric distribution but limits itself to the effect of fluids. For this investigation, we use a simplified conceptual model where the sample is treated as a three phase composite consisting of grain material, water, and TCE. The saturated composite can be described by three parameters, compressional wave velocity ($V_{p_{sat}}$), shear wave velocity ($V_{s_{sat}}$), and

[1]Department of Earth, Atmospheric, and Planetary Sciences, Massachusetts Institute of Technology, Cambridge, Massachusetts, USA.
[2]Formerly at Department of Geophysics, Stanford University, Stanford, California, USA.
[3]Earth Science Division, Lawrence Berkeley National Laboratory, Berkeley, California, USA.
[4]Department of Geophysics, Stanford University, Stanford, California, USA.

0094-8276/07/2006GL029200$05.00

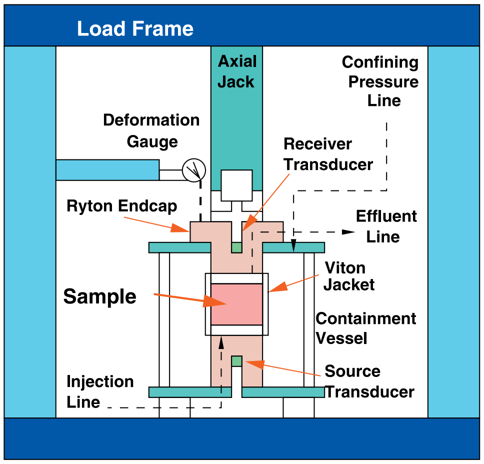

Figure 1. Solvent compatible pressure cell used for pulse transmission measurements. The electronic and fluid handling components of the system are not shown.

bulk density (ρ_{sat}) or equivalently as ρ_{sat} and wet shear and bulk moduli (μ_{sat} and K_{sat}).

1.2. Previous Laboratory Investigations

[6] Several experimental studies have examined the impact of NAPL saturation on ultrasonic properties of synthetic soils. *Geller and Myer* [1995] investigated the relationship between NAPL saturation, P-wave velocity, and attenuation at effective pressures of 140 kPa using 1,1,2-trichloro-1,2,2-trifluro-ethane (freon-113), n-dodecane, and iso-octane as model contaminants using a pulse-transmission apparatus operating at 500 kHz. Reductions in V_p of up to 40.3% were observed for sands fully saturated with freon-113. *Seifert et al.* [1999] performed a similar set of measurements with a focus on varying fluid viscosity and wetting properties. V_p and Q_p were measured while saturating samples with two different grades of silicone oil (10 and 100 cs), castor oil, and n-dodecane at effective pressures of 690 kPa. Both sets of experiments were performed with ultrasonic pulse transmission systems operating between 500 and 1000 kHz. Both *Geller and Myer* [1995] and *Seifert et al.* [1999] made measurements on synthetic samples consisting of medium sub-rounded quartz sand (212-250 microns) with porosities between 35% and 42%.

1.3. A Model For Fluid Substitution

[7] Past efforts to develop rock-physics models for NAPL saturation have met mixed success; methods considered include the Kuster-Toksoz scattering model [*Geller and Myer*, 1995] and the dynamic composite elastic medium model (DYCEM) [*Seifert et al.*, 1999]. *Carcione et al.* [2003] proposed a model for the seismic properties of contaminated sediments based on an extension of Biot-Gassmann theory with the addition of patchy saturation and viscodynamic effects related to clay content.

[8] We adopt a model which combines Gassmann fluid substitution [*Gassmann*, 1951; *Mavko et al.*, 1998] and Hill's equation [*Hill*, 1963] to estimate the seismic signature of TCE injection into water saturated granular media. This approach, sometimes referred to as the Biot-Gassmann-Hill model (BGH) [*Johnson*, 2001], assumes a macroscopic patchy distribution of fluids in contrast to formulations requiring fluid mixing on the pore scale. Although the BGH model neglects dynamic Biot effects, numerical tests indicate that such processes, while present, are small yielding a maximum difference in V_p of 1.2%.

[9] We follow the BGH formulation described by *Dvorkin et al.* [1999] and *Johnson* [2001]. We calculate the bulk and shear moduli of the water saturated fluid/solid composite using measured $V_{p_{sat_w}}$ and ρ_{sat_w} values and a literature estimate of the wet V_p/V_s ratio at a similar pressure; we use a value of 5 obtained from measurements on clean sands carried out by *Zimmer et al.* [2002] at low pressure (<1 MPa). We then estimate the frame bulk modulus (K_{fr}) using the Gassmann model. The Gassmann model assumes that fluids do not effect rock shear properties i.e. $\mu_{fr} = \mu_{sat_w}$. These frame properties, derived from the water-saturated case, serve as a starting point for our model predictions.

[10] Hill's equation [*Hill*, 1963] provides an exact formulation for the properties of a multi-phase composite where all components have identical shear moduli but possibly different bulk moduli. The general form of Hill's equation, which is independent of the geometry of the constituent phases, can be expressed as,

$$K_{eff} = \left(\sum_{i=1}^{n} \frac{x_i}{K_i + \frac{4}{3}\mu} \right)^{-1} - \frac{4}{3}\mu \tag{1}$$

where x_i and K_i are the volume fraction and bulk modulus of the ith phase respectively. In our case, the phases chosen are not the pure fluid or mineral components but different regions where Gassmann's model holds for a single fluid; phase 1 is a fully water saturated composite while phase 2 is fully saturated with TCE. The fraction of phase 1 and 2 are controlled by the measured TCE saturation. The properties of the water/TCE/mineral composite are then estimated by computing the phase 1 and 2 properties using the Gassmann model and the previously estimated frame properties, followed by application of equation 1.

2. Experimental Methods

[11] We measure seismic P-wave velocity using the ultrasonic pulse-transmission method. This well-developed technique [*Wyllie et al.*, 1956] has found broad application in characterizing the seismic properties of granular materials including unconsolidated sediments [*Zimmer et al.*, 2002]. The pulse transmission method measures the time-of-flight of an acoustic pulse traveling across a sample of known length to estimate seismic propagation velocity. Since the pulse traverses the entire sample, the measurement yields a length-averaged velocity in cases where the sample is not uniform.

2.1. Ultrasonic Measurement System

[12] Figure 1 shows a schematic of the pulse measurement system and the triaxial confining cell. The soil sample is jacketed in an impermeable viton elastomer sleeve situated within a containment vessel allowing for application of confining stress. The top and bottom surfaces of the sample are in contact with endcaps constructed from compression molded polyphenylene sulfide (PPS/ryton), a compound with both superior chemical resistance to TCE and a high coupling coefficient with soft granular materials. Each endcap has two injection ports connected to fluid distribu-

Table 1. Summary of Sample Characteristics

Sample	Porosity, Fraction	Sand/ Silt/ Clay, %	V_p, Water Saturated, m/s	Maximum TCE Saturation, Fraction	ΔV_p, %
Synthetic Granular Samples					
Synthetic #1	0.402	100/0/0	1880	0.22	−4.79
Synthetic #2	0.465	100/0/0	1784	0.59	−15.65
Natural Aquifer Samples					
Natural #1	0.34	95/1/4	1776	0.59	−12.16
Natural #2	0.42	62/21/17	1737	0.30	−5.78

tion grooves on the cap face. Mounted within the endcaps are a matching pair of 500 kHz contact transducers (Part # V101, Panametrics, Waltham, MA) used to generate the ultrasonic pulse. The transducers are driven by a high-voltage pulse generator (IRCO, model M1K-20) set to produce a square wave (0.8 μs width, 400 V amplitude). For each measurement, 100 waveforms were stacked and recorded using a digital oscilloscope (Lecroy 9310A). Axial and confining loads were maintained by syringe pumps (model 500 D, Isco Inc.) that operate in constant pressure mode. TCE is injected into the sample using a transfer cylinder driven by a third syringe pump. Changes in sample length are monitored by a deformation gauge mounted on the load frame.

2.2. Sample Acquisition and Preparation

[13] The natural aquifer samples were acquired from the DOE Pinellas site using a rotary sonic drilling system and split into 5 ft. sections ($\approx$1.5 m) before being transported off-site. The cores were initially drained of free water and then split into smaller 7 cm sections followed by sub-coring to a 7 cm diameter. The resulting samples were frozen and placed in a viton jacket before being loaded into the confining cell. Water for saturating the aquifer samples was prepared by equilibrating vacuum deaired DI water with the annulus remaining from the sub-coring process. Although efforts were made to preserve core integrity, disruption of the internal granular framework might have occurred during the acquisition, transport, sub-coring, or freezing processes; the resulting samples should be viewed as representative of the site but are probably not identical to *in situ* materials.

[14] The synthetic samples were composed of glass beads (Potters Ballotini GB8) sieved between standard 60 and 70 meshes (grain diameter $\approx$212 to 250 μm). The beads were rinsed in DI water followed by drainage and air drying. After drying, 250 g of beads were separated, rewetted, and then slowly poured into a water-filled Teflon sleeve pre-mounted on the bottom end cap. The water used for saturating the synthetic samples was pre-equilibrated with the same type of glass beads.

2.3. Procedure

[15] The natural samples, after being loaded into the confining cell as described above, were slowly flooded with equilibrated water. Injection pore pressure was incrementally increased to a maximum of 350 kPa while adjusting axial and confining pressures to maintain relatively constant effective stress conditions. During the water saturation process, the amplitude of the P-wave first arrival gradually increased; the sample was considered fully water saturated when the waveform achieved a steady state.

[16] TCE, dyed red (Oil Red O Dye, Sigma Aldrich) for visibility, was then slowly injected from the bottom of the sample to minimize density-driven flow instabilities. Flow rates were estimated from both the injection pump indicator and the mass changes of the collected effluent column. When flow rates decreased to near zero, the injection pressure was increased followed by a corresponding increase in confining pressure to maintain near-constant effective stress conditions. Ultrasonic waveforms were acquired during the injection process. Injection continued until injection pressures exceeded 280 kPa, indicating difficulty in displacing the remaining pore water. P-wave first arrival times were determined by picking the first zero-crossing. De-aired DI water was used as the calibration fluid.

[17] Following the experiments, the samples were excavated to qualitatively ascertain TCE distribution and oven-dried at 105°C to determine the dry samples mass. Mean grain density was determined on small sub-samples using a pycnometer-type measurement. Total porosity was calculated from dry sample mass, the measured grain density of the solid, and the sample volume while in the measurement apparatus. For the natural samples, sand/silt/clay fractions were determined through hydrometer sedimentation analysis of 100g samples.

3. Results and Discussion

[18] Table 1 summarizes the basic sample properties including porosity and sand/silt/clay fraction in addition to the effective stress state and the maximum departure in V_p observed during the injection process. All four of the samples had high porosities ($0.34 \leq \phi \leq 0.465$). V_p values in the initial state were typical for unconsolidated sands at these effective stress levels (1740 m/s $\leq V_p \leq$ 1880 m/s) and were not strongly correlated with either porosity or texture. Among the natural aquifer samples, sample # 1 was a clean sand while sample # 2 was a sandy loam. The maximum TCE saturation achieved before break-through varied between 0.22% and 0.59%.

[19] Figure 2 (see Tables S1–S4 of the auxiliary material)[1] shows V_p as a function of TCE saturation for both the natural aquifer (Figure 2a) and the synthetic (Figure 2b) samples. All four experiments observed an approximately linear decrease in V_p during saturation with maximum reductions of between 4.79 and 15.65% from water saturated values. Although the transducers had a resonant frequency of 500 kHz, spectral analysis of recorded waveforms indicated a central frequency closer to 250 kHz for transmitted arrivals.

[20] The measurements for all samples were compared to the BGH model predictions, shown as solid lines on Figure 2. In the absence of quantitative grain mineralogy measurements, we assumed that natural aquifer grains had the properties of quartz (ρ_g = 2650 kg/m^3, $K_g = 36 \times 10^9$ Pa, $\mu_g = 45 \times 10^9$ Pa) as compiled by *Mavko et al.* [1998]; visual examination of the sand fraction suggests that quartz is indeed the dominant component. For the

[1]Auxiliary material data sets are available at ftp://ftp.agu.org/apend/gl/2006gl029200. Other auxiliary material files are in the HTML.

experiments on synthetic bead samples, the properties of soda lime glass were used for the required grain parameters (ρ_g = 2530 kg/m^3, K_g = 43 $\times$ 10^9 Pa, μ_g = 30 $\times$ 10^9 Pa). Since frame properties are computed from the water saturated end-points, all BGH curves are "anchored" to these values. While the BGH predictions provided a qualitative match to the data, they systematically underestimated the decrease in V_p due to TCE saturation for both types of samples. These discrepancies were particularly visible at the high saturations achieved during the 1st natural and 2nd synthetic experiments. Considering the simplicity of the BGH model, this disagreement is not entirely surprising and could be due to non-Gassmann behavior such as changes in frame shear properties induced by TCE saturation. Small uncompensated perturbations in pore pressure might also result in frame property modifications during injection. Simultaneous measurement of V_s, although not possible using our apparatus, would allow calculation of changes in wet frame properties and quantification of shear modulus variations.

[21] One alternative to plotting V_p in terms of saturation is to convert measured values to TCE volume fractions, the ratio of TCE volume to total sample volume, and relative changes in velocity, a step which normalizes for differences in porosity and baseline frame properties. Figure 3 shows the % change in V_p as a function of TCE volume fraction (F_{TCE}) with a linear fit to all measurements shown in cyan. In this case, the fit takes the form $\Delta V_p\% = 0.4519 - 56.87\ F_{TCE}$ and, although empirical, provides an excellent match with the complete dataset.

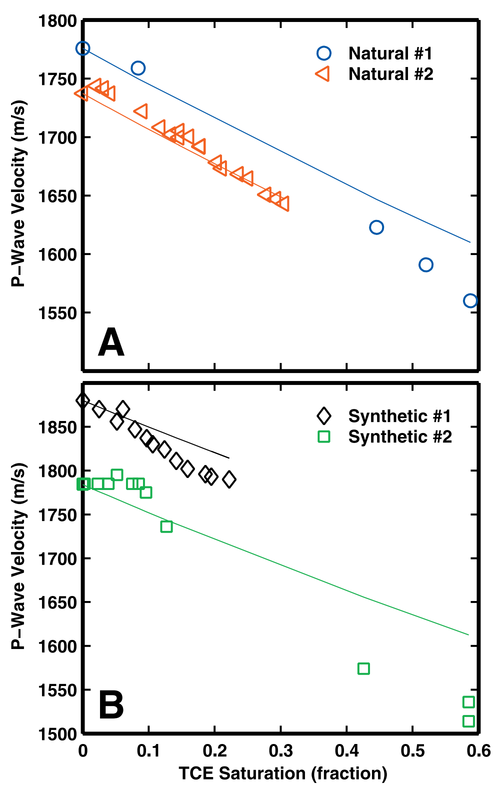

Figure 2. P-wave velocity as a function of TCE saturation. (a) Results for the two natural aquifer samples. (b) Equivalent results for two synthetic samples. The solid lines indicate the BGH model predictions.

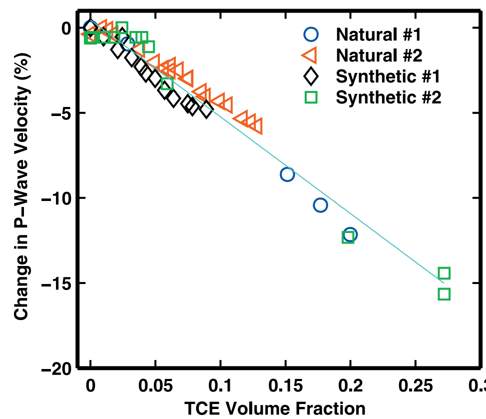

Figure 3. Percent change in P-wave velocity as a function of TCE volume fraction. The cyan line is a linear fit to all available relative measurements.

[22] In addition to the measured variations in ultrasonic arrival time, decreases in signal amplitude and frequency content were also observed during TCE injection. A detailed analysis of these attenuation phenomena will be the focus of future research.

4. Conclusion

[23] The ultrasonic properties we have measured provide a starting point for estimating the seismic signature of TCE pools or similar dense contaminants *in situ*. Recent CPT-based sampling of DNAPL contaminant pools by *Parker et al.* [2003] observed layers with peak saturations near 50%, levels sufficient to yield reductions in V_p on the order of 150 m/s assuming the validity of our empirical model. Unfortunately, the same study estimated the thickness of the high saturation region to be between 5 and 15 cm, suggesting that spatial resolution rather than sensitivity will constrain the seismic delineation of DNAPL regions. Equally problematic for characterization efforts are issues of non-uniqueness; a similar reduction in V_p could be generated by a variety of other subsurface processes including biogenic gas production tied to zones of residual contamination. One approach to resolving issues of non-uniqueness is the introduction of auxiliary datasets, either secondary parameters extracted from the seismic waveform such as attenuation, or unrelated geophysical measurements with sensitivity to the presence of DNAPLs with ground penetrating radar [*Ajo-Franklin et al.*, 2004] being a likely candidate.

[24] **Acknowledgments.** The first and second authors contributed equally to this work. The first author would like to thank M.N. Toksöz, the Founding Members Consortium of the Earth Resources Laboratory, and the EPA's STAR Fellowship program for their generous support and guidance. Elements of this research were supported by DOE grant DE-AC-03-76F0098 under the Subsurface Contamination Focus Area of the Environmental Management Program. We would also like to thank the DOE Pinellas staff and Ken Williams for project assistance.

References

Ajo-Franklin, J. B., J. T. Geller, and J. M. Harris (2004), The dielectric properties of granular media saturated with DNAPL/water mixtures, *Geophys. Res. Lett.*, *31*, L17501, doi:10.1029/2004GL020672.

Biot, M. (1956), Theory of propagation of elastic waves in fluid saturated porous solids: 1. Low frequency range, *J. Acoust. Soc. Am.*, *28*, 168–191.

Carcione, J., G. Seriani, and D. Gei (2003), Acoustic and electromagnetic properties of soils saturated with salt water and NAPL, *J. Appl. Geophys.*, *52*, 177–191.

Dvorkin, J., D. Moos, J. Packwood, and A. Nur (1999), Identifying patchy saturation from well logs, *Geophysics*, *64*, 1756–1759.

Gassmann, F. (1951), Über die Elastizität poröser Medien, *Veirteljahrsschr. Nat. Ges. Zürich*, *96*, 1–23.

Geller, J., and L. Myer (1995), Ultrasonic imaging of organic liquid contaminants in unconsolidated porous media, *Contam. Hydrol.*, *19*, 85–104.

Hill, R. (1963), Elastic properties of reinforced solids: Some theoretical principles, *J. Mech. Phys. Solids*, *11*, 357–372.

Johnson, D. L. (2001), Theory of frequency dependent acoustics in patchy-saturated porous media, *J. Acoust. Soc. Am.*, *110*, 682–694.

Mavko, G., T. Mukerji, and J. Dvorkin (1998), *The Rock Physics Handbook: Tools for Seismic Analysis in Porous Media*, Cambridge Univ. Press, New York.

Mercer, J., and R. Cohen (1990), A review of immiscible fluids in the subsurface: Properties, models, characterization, and remediation, *Contam. Hydrol.*, *6*, 107–163.

Montgomery, J. (1991), *Groundwater Chemicals Field Guide*, Lewis Publ., Chelsea, Mich.

Nath, J., and R. Saini (1990), Ultrasonic and dielectric behavior of binary systems of methyl ethyl ketone with 1,2-dichloroethane, methylene chloride, trichloroethene, tetrachloroethene, and cyclohexane, *J. Chem. Soc. Faraday Trans.*, *86*(4), 645–650.

Pankow, J., and J. Cherry (1996), *Dense Chlorinated Solvents and Other DNAPLs in Groundwater*, Waterloo Press, Portland, Oreg.

Parker, B., J. Cherry, S. Chapman, and M. Guilbeault (2003), Review and analysis of chlorinated solvent dense nonaqueous phase liquid distributions in five sandy aquifers, *Vadose Zone J.*, *2*, 117–137.

Romig, P. (Ed.) (2000), *Seeing Into the Earth: Noninvasive Characterization of the Shallow Subsurface for Environmental and Engineering Application*, Natl. Acad. Press, Washington, D. C.

Seifert, P., B. Kaelin, and L. Johnson (1999), Effect on ultrasonic signals of viscous pore fluids in unconsolidated sand, *J. Acoust. Soc. Am.*, *106*, 3089–3094.

Temples, T., M. Waddel, W. Domoracki, and J. Eyer (2001), Noninvasive determination of the location and distribution of DNAPLs using advanced seismic reflection techniques, *Groundwater*, *39*, 465–474.

Wyllie, M., A. Gregory, and L. Gardner (1956), Elastic wave velocities in heterogeneous and porous media, *Geophysics*, *21*, 41–70.

Zimmer, M., M. Prasad, and G. Mavko (2002), Pressure and porosity influences on V_p - V_s ratios in unconsolidated sands, *Leading Edge*, *21*, 178–183.

J. B. Ajo-Franklin, Department of Earth, Atmospheric, and Planetary Sciences, Massachusetts Institute of Technology, E34-566, 42 Carleton Street, Cambridge, MA 022142, USA. (jfrank@erl.mit.edu)

J. T. Geller, Earth Science Division, Lawrence Berkeley National Laboratory, 1 Cyclotron Road, Building 50E, Mailstop 90R116, Berkeley, CA 94720, USA.

J. M. Harris, Department of Geophysics, Stanford University, 397 Panama Mall, Stanford, CA 94305, USA.